Research Square

Preprints are preliminary reports that have not undergone peer review.
They should not be considered conclusive, used to inform clinical practice,
or referenced by the media as validated information.

Agreement Between the Advanced Vision Analyzer Virtual Reality Perimeter and the Octopus 101 in Glaucoma Patients

Liamet Fernández Argones

liamet.fernandez@gmail.com

Cuban Institute of Ophthalmology Ramón Pando Ferrer

Yunet Regla Campos Borges

Cuban Institute of Ophthalmology Ramón Pando Ferrer

Ibrain Piloto Díaz

Cuban Institute of Ophthalmology Ramón Pando Ferrer

Elizabeth Bárbara Cuétara Lugo

Cuban Institute of Ophthalmology Ramón Pando Ferrer

Francisco Yunier Fumero González

Cuban Institute of Ophthalmology Ramón Pando Ferrer

Andrés Queupumil Rodríguez

Cuban Institute of Ophthalmology Ramón Pando Ferrer

Inalvis Suárez Cuza

Cuban Institute of Ophthalmology Ramón Pando Ferrer

Research Article

Keywords: virtual reality perimetry, Advanced Vision Analyzer, primary open-angle glaucoma

Posted Date: May 28th, 2026

DOI: https://doi.org/10.21203/rs.3.rs-9383318/v1

License: This work is licensed under a Creative Commons Attribution 4.0 International License.
Read Full License

Additional Declarations: No competing interests reported.

Abstract

Purpose

to evaluate the agreement and reliability of sensitivity measurements obtained with the AVA virtual reality perimeter compared to conventional Octopus 101 perimeter in patients with glaucoma.

Methods

A cross-sectional pilot study was conducted in 24 patients with stable glaucoma. Perimetric examinations were performed using AVA (Elisar Fast strategy) and Octopus 101 (TOP strategy). Levels of agreement were analyzed for global, sectorial, and pointwise sensitivity, as well as for the detection of topographic defects and classification according to the Glaucoma Staging System 2.

Results

Global sensitivity showed strong correlation and good reliability (rho = 0.78; ICC = 0.85), as did sectorial sensitivity by eccentricity (rho = 0.85; ICC = 0.80), while pointwise sensitivity was moderate (rho = 0.50; ICC = 0.64). Bland–Altman analysis of global sensitivity revealed a mean bias of 0.057 dB and limits of agreement between − 0.129 and 0.243 dB, with no significant proportional bias. Detection of topographic defects coincided in 50% of cases, with moderate agreement (kappa = 0.483; 95% CI: 0.23–0.74). Ninety-two percent of cases corresponded to stage S1 or lower, with weak agreement in glaucoma staging (kappa = 0.327; 95% CI: 0.03–0.62; p = 0.038).

Conclusions

The AVA perimeter demonstrates solid agreement at global and sectorial levels, with moderate pointwise consistency compared to Octopus 101, supporting its clinical applicability in glaucoma. Its ability to detect topographic defects and classify disease severity is acceptable, though algorithmic adjustments and normative cut-offs may enhance performance. Longitudinal studies with larger sample sizes and healthy control groups are recommended to validate and optimize its utility.

Key points

1- AVA demonstrated consistently higher pointwise sensitivity values within the central 30° visual field, while maintaining strong concordance with Octopus 101, enhancing its potential applicability in routine clinical practice.

2- Both devices showed strong correlations and good reliability across global and sectoral analyses, with minimal bias; however, they should not be considered interchangeable for longitudinal patient follow-up.

3- Glaucoma Staging System 2 severity classification revealed only fair agreement between AVA and Octopus, highlighting the need for specific cut-off values tailored to virtual reality perimeters for consistent clinical staging.

Introduction

Glaucoma is the leading cause of irreversible blindness worldwide, affecting more than 79.6 million people in 2020, with projections indicating an increase to 111.8 million cases by 2040. Standard automated perimetry remains an essential tool for detecting functional alterations in glaucoma patients, as well as the reference method for determining disease severity, estimating prognosis, and monitoring progression over time. [1–3]

Several studies have suggested that virtual reality devices, such as the Advanced Vision Analyzer (AVA), may provide performance comparable to, or even superior in certain parameters, to conventional perimetry. However, there remains a need to validate the agreement between both technologies, particularly regarding visual field sensitivity and glaucoma damage staging. Such validation would support the consolidation of more precise and effective diagnostic strategies, ultimately contributing to improved prevention of progression toward irreversible blindness. [4, 5]

The objective of this study was to evaluate the agreement and reliability of sensitivity measurements obtained with the AVA virtual reality perimeter compared to those acquired with the conventional Octopus 101 perimeter in patients with glaucoma. Furthermore, the study assessed concordance in the detection of topographic defects and in the classification of glaucoma severity. The Octopus 101 is often the device available in clinical practice in many developing countries.

Methods

A cross-sectional, observational, and analytical pilot study was conducted in 24 right eyes of 24 patients diagnosed with primary open angle glaucoma who attended the Glaucoma Department of the Cuban Institute of Ophthalmology “Ramón Pando Ferrer” between January 2023 and January 2024. Inclusion criteria comprised patients over 40 years of age with aided monocular distance visual acuity ≤ 0.20 logMAR (6/9.5 Snellen) and otherwise normal ophthalmological examination, except for findings consistent with primary open-angle glaucoma. Exclusion criteria included history of ocular trauma, previous ocular surgery, systemic diseases with ocular involvement, refractive error greater than 5 spherical diopters or 2 cylindrical diopters, coexistence of neuro-ophthalmological disorders or other conditions that could independently explain visual field alterations, and unreliable tests with more than 25% false positives, false negatives, or fixation losses.

Glaucoma diagnosis was defined by intraocular pressure > 21 mmHg and the presence of glaucomatous optic neuropathy or visual field findings. Glaucomatous optic neuropathy was defined by the presence of generalized, wedge-shaped, or slit-like defects of the retinal nerve fiber layer in the superotemporal or inferotemporal sectors; generalized or sectoral thinning of the neuroretinal rim; a cup to disc ratio greater

than 0.5; or an interocular asymmetry exceeding 0.2. A visual field was classified as glaucomatous if at least three contiguous points within the central 30° were affected, with at least one showing a probability of less than 1% in the normal population, and if the defect exhibited a typical pattern consistent with the distribution of the retinal nerve fiber bundles.

All patients underwent interview and complete ophthalmological examination according to the hospital protocol for glaucoma care. For visual field testing, two devices were used: the AVA virtual reality perimeter and the conventional Octopus 101 perimeter. All examinations were performed by an experienced optometrist in a dark room, with perimeter calibration according to manufacturer standards and continuous monitoring of central fixation. The first test was performed with the Octopus 101 perimeter, corresponding to routine clinical follow-up (TOP strategy, program 32). After one hour, patients were evaluated with the AVA perimeter (Elisar Fast strategy, 24-2 pattern). In patients under glaucoma follow-up, a single visual field test was performed, while newly diagnosed cases underwent two evaluations. Reliability indices and scotoma topography were corroborated in each case.

The AVA perimeter consists of four main components: a virtual reality headset, a patient response button, an operator control device, and a cloud server for storing examinations. The headset incorporates an optical system and a liquid crystal display. The screen is coupled to convex lenses that present a magnified virtual image at 60 cm, observed during the test. The device is dichoptic, presenting images to each eye without requiring occlusion, and can also be performed binocularly. Eyetracking is achieved through two infrared cameras, one for each eye, and an infrared LED system to illuminate the pupil. Pupil images are wirelessly transmitted to the operator's device. This technology employs the Elisar Standard Algorithm (ESA), with a normative database of 100 patients, to determine threshold values within normal limits. [6]

The TOP strategy of the Octopus 101 perimeter (Haag-Streit International) uses mathematical extrapolation after testing each visual field point once, with Goldmann III stimulus size, 100 ms duration, and background luminance of four apostilbs. The normative database was established from a multicenter study conducted in 1985 including approximately 350 normal subjects. [7]

Agreement between technologies was evaluated for mean sensitivity at the global level, across visual field zones according to eccentricity, pointwise and within the sectors corresponding to the Glaucoma Hemifield Test (GHT) (Figure 1). Agreement was not determined for mean defect and loss variance due to inherent differences between technologies. Specifically, the Octopus 101 calculated mean defect from 74 locations and did not generate measurements when point defect reached 5 dB, representing a methodological limitation for this study.

The Spearman's rho was categorized according to Schober et al. [8]: < 0.10, negligible; 0.10–0.39, weak; 0.40–0.69, moderate; 0.70–0.89, strong; > 0.90, very strong. Reliability was assessed using the intraclass correlation coefficient (ICC) following Koo and Li [9]: < 0.50, poor; 0.50–0.74, moderate; 0.75–0.90, good; > 0.90, excellent. Concordance was analyzed using the Bland–Altman method, with natural logarithmic transformation of mean values to reduce variability and improve distribution symmetry. Kappa index was

interpreted according to Landis and Koch [10]: 0, poor; 0.01–0.20, slight; 0.21–0.40, fair; 0.41–0.60, moderate; 0.61–0.80, substantial; > 0.80, almost perfect.

This study was approved by the Scientific Council and Research Ethics Committee of the Cuban Institute of Ophthalmology Ramón Pando Ferrer. Informed consent was obtained from all participants for the use of their data in scientific research, in accordance with the Declaration of Helsinki. [11]

Results

Data were obtained from 24 patients with a mean age of 59 years, of whom 70% were women and 62% Caucasian. The mean sensitivity measured with the AVA perimeter was significantly higher than that obtained with the Octopus 101, globally (1.5 ± 2.2 dB; $p < 0.05$) as well as in the 10–20° (1.8 ± 2.6 dB) and 20–30° (1.6 ± 2.2 dB) zones. No significant differences were found in the central 0–10° zone (0.8 ± 2.3 dB) or in global mean defect (0.3 ± 2.4 dB). The mean examination duration exceeded five minutes with the AVA Elisar Fast strategy, whereas it was less than four minutes with the Octopus 101 TOP strategy ($p < 0.001$). (Table 1)

The mean global sensitivity measured with AVA showed a strong positive correlation with Octopus 101 (rho = 0.78; $p < 0.001$; 95% CI: 0.55–0.90). The reliability between both technologies was good (ICC = 0.85; $p < 0.001$; 95% CI: 0.65–0.94). The Bland–Altman analysis of log-transformed mean sensitivity revealed a mean bias of 0.06 and limits of agreement between –0.13 and 0.24, with 96% of points within limits. The regression analysis of differences versus means showed no evidence of proportional bias (B = 0.06; $p = 0.711$), indicating stable agreement across values. These findings support adequate concordance between technologies, independent of measurement magnitude, validating AVA's clinical applicability for visual field sensitivity assessment.

Across the three eccentricity zones, strong and statistically significant correlations were observed between the two technologies (rho = 0.77, 0.70, and 0.72; $p < 0.001$, from center to periphery). The reliability was good, with ICC values of 0.85 (95% CI: 0.66–0.94), 0.80 (0.54–0.91), and 0.84 (0.62–0.93), all $p < 0.001$. The Bland–Altman analysis of log-transformed sensitivity values across visual field zones showed small mean biases (0.03–0.07) with 95% limits of agreement (–0.15 to 0.29). The regression slopes were non-significant ($p > 0.05$), confirming the absence of proportional bias and the stability of differences between AVA and Octopus across sensitivity levels.

At individual locations, Figures 2a and 2b show that AVA sensitivity averages exceeded Octopus 101 by 0–4 dB (mean 1.5 0.9 dB). Figures 2c and 2d show absolute differences ranging from 2–5 dB (mean 3.3 ± 0.6 dB). These findings indicate that although variability existed among individuals at some points, discrepancies remained within clinically acceptable ranges.

Table 1. Demographic and perimetric characteristics of the study sample

Characteristic		Range (Min-Max)	Mean (SD)	p*
Age (years)		44 to 75	59 (9)	NA
Mean sensitivity globally (dB)	**AVA**	20 to 31	26.5 (3.2)	**0.004**
	Octopus	16 to 29	25.0 (2.8)	
Mean sensitivity 0-10º (dB)	**AVA**	19 to 32	27.5 (3.4)	0.098
	Octopus	19 to 31	26.7 (2.9)	
Mean sensitivity 10-20º (dB)	**AVA**	18 to 31	26.8 (3.4)	**0.002**
	Octopus	16 to 29	25.0 (3.0)	
Mean sensitivity 20-30º (dB)	**AVA**	19 to 30	25.4 (3.0)	**0.004**
	Octopus	15 to 28	23.8 (2.9)	
Mean defect (dB)	**AVA**	-9.4 to 1.1	-1.8 (2.9)	0.209
	Octopus	-11.5 to 1.1	-2.1 (2.6)	
PSD (dB)		-3.4 to 5.4	2.5 (1.6)	NA
LV (dB)		-7.9 to 15.3	5.6 (5.2)	NA
Mean duration (minutes)	**AVA**	3.7 to 9.0	5.2 (1.2)	**p< 0.001**
	Octopus	2.1 to 10.4	3.5 (2.2)	

Min: minimum; Max: maximum; SD: Standard deviation; NA: not applicable (variables not compared between devices); AVA: Advanced Vision Analyzer; dB: decibels; PSD: Pattern standard deviation; LV: Loss variance.

*: Wilcoxon signed-rank test

The similar pointwise mean sensitivity between AVA and Octopus, with low differences and variability, suggests good agreement in most locations, particularly in central zones. This figure supports the utility of AVA as a functional assessment tool in clinical settings, with no evidence of systematic bias

The Figure 3a shows that in 83% of locations, threshold sensitivity measured with AVA correlated moderately to strongly with Octopus 101 (rho = 0.42–0.79; $p < 0.05$), with mean rho of 0.50. In 77.8% of locations (Figure 3b), pointwise sensitivity measurements were consistent between technologies (ICC > 0.50; $p < 0.05$). Seven locations (13%) achieved good reliability (ICC = 0.76–0.85; $p < 0.05$). The overall mean ICC was 0.64, indicating moderate consistency across all locations.

With AVA, the mean sensitivity showed a moderate inverse correlation with examination duration, indicating that patients with better sensitivity completed the test faster (rho = –0.60; $p = 0.002$). Conversely, greater mean defect was associated with longer test times (moderate direct correlation, rho

= 0.54; p = 0.007), and higher pattern deviation also correlated with longer durations (rho = 0.44; p = 0.034). This suggests that more impaired visual function results in longer test times. In contrast, the Octopus perimeter showed no significant association between test duration and measures of visual function, indicating that examination time was not influenced by visual field status.

The analysis of defect detection showed moderate agreement between AVA and Octopus 101. In 45.8% of cases (11/24), both technologies agreed on absence of topographic defects, while one case showed a central defect detected by both. A nasal step was detected by AVA in three cases and by Octopus in four. Superior, inferior, or combined arcuate defects showed partial agreement, with AVA detecting more cases. Cohen's kappa was 0.48 (95% CI: 0.23–0.74), indicating moderate agreement in identifying glaucomatous patterns.

Evaluation of GHT sectors showed that AVA yielded higher mean sensitivity in all sectors, with significant differences ($p < 0.05$) in sectors 3 (superior and inferior), 4 (superior and inferior), and 5 superior (Table 2). Spearman's rho coefficients evidenced significant correlations ($p < 0.05$) across all sectors, predominantly moderate to strong, suggesting high functional concordance between devices in regions typically affected by glaucoma (Figure 4). Inferior sectors 1 and 2 showed the highest correlations (rho = 0.76–0.80). In contrast, superior sector 5 presented the lowest correlation (rho = 0.53), which may reflect anatomical variability or reduced agreement in less compromised zones. The reliability was good across all sectors (ICC = 0.76–0.87), except for sector 5 inferior, which was moderate.

The Bland–Altman analysis showed that 92–100% of points fell within the limits of agreement across GHT sectors. Regression analysis confirmed stable concordance without proportional bias in most zones. In superior sector 1 and inferior sector 3, proportional bias was statistically significant, suggesting that AVA may overestimate sensitivity at higher values compared to Octopus. However, the low coefficients of determination ($R^2 = 0.21$ and 0.17) indicate that this bias accounted for only a small fraction of the differences between devices. The remaining variability is likely influenced by uncontrolled factors such as stimulus design, fatigue, virtual environment conditions, or learning effects. Overall, both technologies demonstrated moderate agreement; however, they should not be considered interchangeable for longitudinal follow-up of the same patient.

Regarding glaucoma severity according to the Glaucoma Staging System 2, 87.5% of patients (21 cases) were classified as stage S1 or lower with the conventional Octopus 101 perimeter, while 91.7% (22 cases) were classified similarly with the AVA perimeter. Both devices coincided in the same stage in 13 patients (54.2%). Cohen's kappa index was 0.33 (95% CI: 0.03–0.62; p = 0.038), indicating fair agreement in the assessment of glaucoma severity.

Table 2. Mean sensitivity in sectors of the Glaucoma hemifield test: AVA–Octopus comparison

GHT sectors		Mean sensibility dB (SD)	Mean difference† dB (SD) (CI 95%, Min-Max)	p*
Superior 1 (central)	**AVA**	27.5 (4.1)	0.3 (3.2) (-1.1 to 1.6)	0.660
	Octopus	27.2 (3.1)		
Inferior 1 (central)	**AVA**	28.5 (3.2)	0.2 (2.5) (-1.2 to 0.9)	0.745
	Octopus	25.6 (3.0)		
Superior 2 (paracentral)	**AVA**	26.8 (3.6)	1.2 (2.8) (-0.1 to 2.4)	0.056
	Octopus	25.6 (3.0)		
Inferior 2 (paracentral)	**AVA**	27.7 (4.1)	1.0 (2.7) (-0.1 to 2.2)	0.068
	Octopus	23.6 (3.7)		
Superior 3 (nasal)	**AVA**	26.0 (2.8)	2.4 (2.8) (1.2 to 3.5)	**p<0.001**
	Octopus	23.7 (3.4)		
Inferior 3 (nasal)	**AVA**	26.7 (3.1)	2.5 (2.8) (1.4 to 3.7)	**p<0.001**
	Octopus	24.1 (3.8)		
Superior 4 (arcuate)	**AVA**	25.4 (2.9)	2.4 (2.5) (1.3 to 3.4)	**p<0.001**
	Octopus	23.0 (3.3)		
Inferior 4 (arcuate)	**AVA**	26.9 (3.9)	1.3 (3.0) (0.1 to 2.5)	**0.044**
	Octopus	25.6 (3.2)		
Superior 5 (arcuate)	**AVA**	24.5 (4.2)	1.7 (3.6) (0.1 to 3.2)	**0.033**
	Octopus	22.8 (3.1)		
Inferior 5 (arcuate)	**AVA**	27.3 (3.4)	1.0 (2.9) (-0.2 to 2.2)	0.107
	Octopus	26.3 (3.0)		

GHT: *Glaucoma Hemifield Test;* dB: decibels; SD: Standard deviation; CI: Confidence interval

†: *Mean difference in sectoral sensitivity (AVA − Octopus) across homologous regions*; *: Wilcoxon signed-rank test

Discussion

This study represents the first comparative analysis between the AVA virtual reality perimeter and the conventional Octopus 101 perimeter, both equipped with rapid strategies that balance diagnostic accuracy and operational efficiency in specialized glaucoma management. Results demonstrate that

AVA provides solid agreement at both global and sectorial levels compared with the conventional standard, supporting its clinical utility. The moderate consistency in pointwise analysis, consistent with the inherent topographic variability of the visual field, together with the absence of proportional bias and stability of differences across measurement magnitudes, reinforces the technical validity of the AVA device.

Previous studies have reported both overestimations [12, 13] and underestimations [6, 14] when comparing virtual reality platforms with conventional perimeters, highlighting heterogeneity among devices and algorithms. Stronger correlations than those observed in the present study have been described in patients with moderate or advanced glaucoma (rho ≈ 0.80), where sensitivity curves are more linear within the 5–25 dB range. In contrast, in healthy eyes, ceiling effects limit response variability and reduce correlation strength (rho = 0.50–0.67). [14, 15]

At the sectorial level, this study shows good correlation in most sectors, except in peripheral regions such as the superior nasal retina. This discrepancy may be attributed to functional preservation of these regions in early stages or technical limitations of the headset in stimulating peripheral zones. [12]

Pointwise variability between devices, as reported by Phu et al. [16], may depend on factors such as attention, fatigue, background luminance, and differences in thresholding strategies. While global metrics average fluctuations, pointwise measures are more sensitive to these effects. In this context, AVA employs low luminance levels, potentially activating mesopic as well as photopic pathways, which may influence stimulus perception and recorded sensitivity. Differences in optical design and algorithms also explain part of this variability: AVA uses an aspheric lens projecting to infinity and the ESA strategy combining adaptive staircase and eye tracking; HFA employs SITA with real-time filtering; and Octopus 101 implements TOP based on normative population thresholds with progressive adjustments. Although effective, these strategies may generate inconsistencies when compared directly or alternated between successive examinations. Unreliable visual fields may increase up to 16% with rapid strategies, particularly in cases of low sensitivity. [6, 7, 13, 17]

Examination time is also affected by the degree of visual damage, with adaptive algorithms such as ESA prolonging duration when sensitivity is low, while TOP maintains more stable timing. This difference suggests that AVA accurately reflects functional impairment, although its efficiency could be optimized through algorithmic improvements. [18] Regarding defect detection, some studies have reported inferior performance of virtual reality devices compared with conventional perimetry. [12, 16] However, the present results show that AVA demonstrates comparable capacity to identify functional alterations. Longer test duration compared with TOP may have facilitated detection of subtle defects.

Topographic analysis revealed a higher prevalence of alterations in the superior hemifield, consistent with previous reports. [19–21] This pattern reflects structural vulnerability of the inferior temporal retina, with greater exposure to glaucomatous damage due to higher fiber density from the inferior macula. According to Hood et al. [22], this zone represents a critical area for early detection, consistent with AVA findings and reinforcing the functional validity of observed defects.

Regarding staging classification, regular agreement was observed, consistent with reports by Greenfield and Mees. [23, 24] These differences may be attributed to distinct normative databases, as AVA employs data generated under specific virtual environment conditions, including background luminance. In this context, proposals such as those by Bradley et al. [25], who adjusted mean defect cut-offs for virtual reality (–5 dB and – 8 dB) and improved concordance with HFA, open the possibility of harmonizing criteria and enhancing classification across platforms.

Overall, the results of this study align with the literature in showing that conventional and virtual reality systems present good correlation, though not full interchangeability. Differences may be explained by factors such as adaptation thresholds, spatial summation (Ricco's law), signal detection theory, and variability among normative databases, underscoring the need to interpret clinical results within the technological context of each tool. [26–28]

Previous studies have shown variability in virtual reality examination times depending on device, algorithm, and patient type. While Narang and Razeghinejad [6, 15] reported longer times with virtual reality, other authors such as Berneshawi and Bradley [12, 25] observed reductions or similar durations compared with HFA. This behavior may depend on the degree of visual damage, as algorithms such as RATA are shorter in patients with extensive scotomas, requiring fewer presentations to define low thresholds. This suggests that optimized headsets may offer specific advantages in monitoring advanced defects. [25]

Virtual reality perimetry presents several strengths that may favor its clinical adoption. AVA allows free head movements during testing, improving patient comfort. Its portable design facilitates extra-hospital monitoring, as demonstrated by Hu et al. [29] in home-based testing with high acceptance. Users also reported the experience as clearer and more understandable, potentially enhancing adherence, particularly in limited-access settings. [30]

Study limitations include the small sample size and absence of a healthy control group, restricting generalizability of findings. Additionally, although AVA compensates for head movements via gyroscope, it lacks active eye tracking, which may require frequent postural adjustments and cause fatigue in patients with limited mobility. Focal discrepancies in defect detection were also observed, suggesting the need for more detailed regional functional analysis.

In conclusion, this study demonstrates that the AVA virtual reality perimeter achieves solid agreement at global and sectorial levels compared with the conventional standard, as well as moderate consistency in pointwise comparison, without biases attributable to measurement magnitude. It has also shown capacity to identify characteristic glaucomatous patterns, supporting its applicability in clinical practice. Nevertheless, longitudinal studies including healthy controls and larger samples, together with cost-effectiveness, durability, and maintenance analyses compared with traditional equipment, will be necessary to consolidate these findings and facilitate systematic implementation.

Declarations

Consent to Publish declaration:

not applicable

Ethics and Consent to Participate declarations:

Written informed consent was obtained from all participants.

Author Contribution

Conceptualization: L.F. and I.P.Clinical procedures and diagnostic testing: L.F., Y.C., A.Q. and I.S.Formal analysis: L.F. and F.F.Data curation: L.F. and Y.C.Methodology: L.F. and E.C.Drafting of the original manuscript: L.F. (all authors reviewed the manuscript)Final writing and editing: L.F.

Data Availability

DeclarationsConsent to Publish declaration: not applicableEthics and Consent to Participate declarations: Written informed consent was obtained from all participants.

References

1. Vision Loss Expert Group of the Global Burden of Disease Study. Global estimates on the number of people blind or visually impaired by glaucoma: a meta-analysis from 2000 to 2020. *Eye*. 2024;38(11):2036–46. https://doi.org/10.1038/s41433-024-02995-5
2. World Health Organization. *World report on vision* [Internet]. Geneva: WHO; 2019. Available from: https://www.who.int/publications/i/item/9789241516570 Accessed 06 Feb 2026
3. Allison K, Patel D, Alabi O. Epidemiology of glaucoma: the past, present, and predictions for the future. *Cureus*. 2020;12(11):e11686. DOI: 10.7759/cureus.11686
4. Selvan K, Mina M, Abdelmeguid H, Gulsha M, Vincent A, Sarhan A. Virtual reality headsets for perimetry testing: a systematic review. *Eye*. 2024;38(6):1041–64.
5. Wong K-A, Ang BCH, Gunasekeran DV, Husain R, Boon J, Vikneson K, et al. Remote perimetry in a virtual reality metaverse environment for out-of-hospital functional eye screening compared against the gold standard Humphrey visual fields perimeter: proof-of-concept pilot study. *J Med Internet Res*. 2023;25:e45044. doi: 10.2196/45044
6. Narang P, Agarwal A, Srinivasan M, Agarwal A. Advanced vision analyzer–virtual reality perimeter: device validation, functional correlation and comparison with Humphrey field analyzer. *Ophthalmology Science*. 2021;1(2):100035. https://doi.org/10.1016/j.xops.2021.100035

7. Racette L, Fischer M, Bebie H, Holló G, Johnson CA, Matsumoto C. *Visual field digest: a guide to perimetry and the Octopus perimeter*. 6th ed. Köniz: Haag-Streit AG; 2016.
8. Schober P, Boer C, Schwarte LA. Correlation coefficients: appropriate use and interpretation. *Anesth Analg*. 2018;126(5):1763–8. DOI: 10.1213/ANE.0000000000002864
9. Koo TK, Li MY. A guideline of selecting and reporting intraclass correlation coefficients for reliability research. *J Chiropr Med*. 2016;15(2):155–63. https://doi.org/10.1016/j.jcm.2016.02.012
10. **Landis JR, Koch GG. An application of hierarchical kappa-type statistics in the assessment of majority agreement among multiple observers. Biometrics. 1977;33(2):363–74.https://doi.org/10.2307/2529786**
11. **World Medical Association. World Medical Association Declaration of Helsinki: ethical principles for medical research involving human participants. JAMA. 2025;333(1):71-74. DOI:10.1001/jama.2024.21972**
12. Berneshawi AR, Shue A, Chang RT. Glaucoma home self-testing using VR visual fields and rebound tonometry versus in-clinic perimetry and Goldmann applanation tonometry: a pilot study. Transl Vis Sci Technol. 2024;13(8):7. doi:https://doi.org/10.1167/tvst.13.8.7
13. Griffin JM, Slagle GT, Vu TA, Eis A, Sponsel WE. Prospective comparison of VisuALL virtual reality perimetry and Humphrey automated perimetry in glaucoma. *J Curr Glaucoma Pract*. 2024;18(1):4–9. doi: 10.5005/jp-journals-10078-1434
14. Stapelfeldt J, Kucur ŞS, Huber N, Höhn R, Sznitman R. Virtual reality–based and conventional visual field examination comparison in healthy and glaucoma patients. *Transl Vis Sci Technol*. 2021;10(12):10. doi:https://doi.org/10.1167/tvst.10.12.10
15. Razeghinejad R, Gonzalez-Garcia A, Myers JS, Katz LJ. Preliminary report on a novel virtual reality perimeter compared with standard automated perimetry. *J Glaucoma*. 2021;30(1):17–23.DOI: 10.1097/IJG.0000000000001670
16. Phu J, Wang H, Kalloniatis M. Comparing a head-mounted virtual reality perimeter and the Humphrey Field Analyzer for visual field testing in healthy and glaucoma patients. *Ophthalmic Physiol O*pt. 2024;44(1):83–95. https://doi.org/10.1111/opo.13229
17. Lee GA, Kong GY, Liu CH. Visual fields in glaucoma: where are we now? Clin Exp Ophthalmol. 2023;51(2):162-9. doi:10.1111/ceo.14217
18. Hekmatjah N, Chibututu C, Han Y, Keenan JD, Oatts JT. Virtual reality perimetry compared to standard automated perimetry in adults with glaucoma: a systematic review. PLoS One. 2025;20(1):e0318074. doi:10.1371/journal.pone.0318074
19. Jiang J, Ye C, Zhang C, Ye W, Wang X, Shang X, et al. Intraocular asymmetry of visual field defects in primary angle-closure glaucoma, high-tension glaucoma, and normal-tension glaucoma in a Chinese population. Sci Rep. 2021;11(1):11674. doi:10.1038/s41598-021-91167-4
20. Park IK, Kim KW, Moon NJ, Shin J-H, Chun YS. Comparison of superior and inferior visual field asymmetry between normal-tension and high-tension glaucoma. *J Glaucoma.* 2021;30(8):648-55. doi:10.1097/IJG.0000000000001823

21. Vandersnickt MF, van Eijgen J, Lemmens S, Stalmans I, Pinto LA, Vandewalle EM. Visual field patterns in glaucoma: a systematic review. *Saudi J Ophthalmol.* 2024;38(4):306-15. doi:10.4103/sjopt.sjopt_146_24
22. Hood DC, Raza AS, de Moraes CG, Liebmann JM, Ritch R. Glaucomatous damage of the macula. *Prog Retin Eye Res.* 2013;32:1-21. doi:10.1016/j.preteyeres.2012.08.002
23. Greenfield JA, Deiner M, Nguyen A, Wollstein G, Damato B, Backus BT, et al. Virtual reality oculokinetic perimetry test reproducibility and relationship to conventional perimetry and OCT. *Ophthalmol Sci.* 2022;2(1):100105. doi:10.1016/j.xops.2022.100105
24. Mees L, Upadhyaya S, Kumar P, Kotawala S, Haran S, Rajasekar S, et al. Validation of a head-mounted virtual reality visual field screening device. *J Glaucoma.* 2020;29(2):86-91. doi:10.1097/IJG.0000000000001417
25. Bradley C, Ahmed IIK, Samuelson TW, Chaglasian M, Barnebey H, Radcliffe N, et al. Validation of a wearable virtual reality perimeter for glaucoma staging, the NOVA trial: novel virtual reality field assessment. *Transl Vis Sci Technol.* 2024;13(3):10. doi:10.1167/tvst.13.3.10
26. Choi EY, Li D, Fan Y, Pasquale LR, Shen LQ, Boland MV, et al. Predicting global test–retest variability of visual fields in glaucoma. *Ophthalmol Glaucoma.* 2021;4(4):390-9. doi:10.1016/j.ogla.2021.04.004
27. García Domene MC. Diseño y testeo de un campímetro de umbral incremental por proyección [tesis doctoral]. Alicante: Universitat d'Alacant; 2013. Disponible en: http://hdl.handle.net/10045/35676
28. WuDunn D, Takusagawa HL, Rosdahl JA, Sit AJ, Chopra V, Ou Y, et al. Central visual field testing in early glaucoma: a report by the American Academy of Ophthalmology. *Ophthalmology.* 2024;131(2):240-8. doi:10.1016/j.ophtha.2023.08.014
29. Hu GY, Prasad J, Chen DK, Alcantara-Castillo JC, Patel VN, Al-Aswad LA. Home monitoring of glaucoma using a home tonometer and a novel virtual reality visual field device: acceptability and feasibility. *Ophthalmol Glaucoma.* 2023;6(2):121-8. doi:10.1016/j.ogla.2022.11.004
30. Chia ZK, Kong AW, Turner ML, Saifee M, Damato BE, Backus BT, et al. Assessment of remote training, at-home testing, and test-retest variability of a novel test for clustered virtual reality perimetry. *Ophthalmol Glaucoma.* 2024;7(2):139-47. doi:10.1016/j.ogla.2023.11.002
31. Asman P, Heijl A. Glaucoma hemifield test: automated visual field evaluation. Arch Ophthalmol. 1992;110(6):812-9. doi:10.1001/archopht.1992.01080180060031

Figures

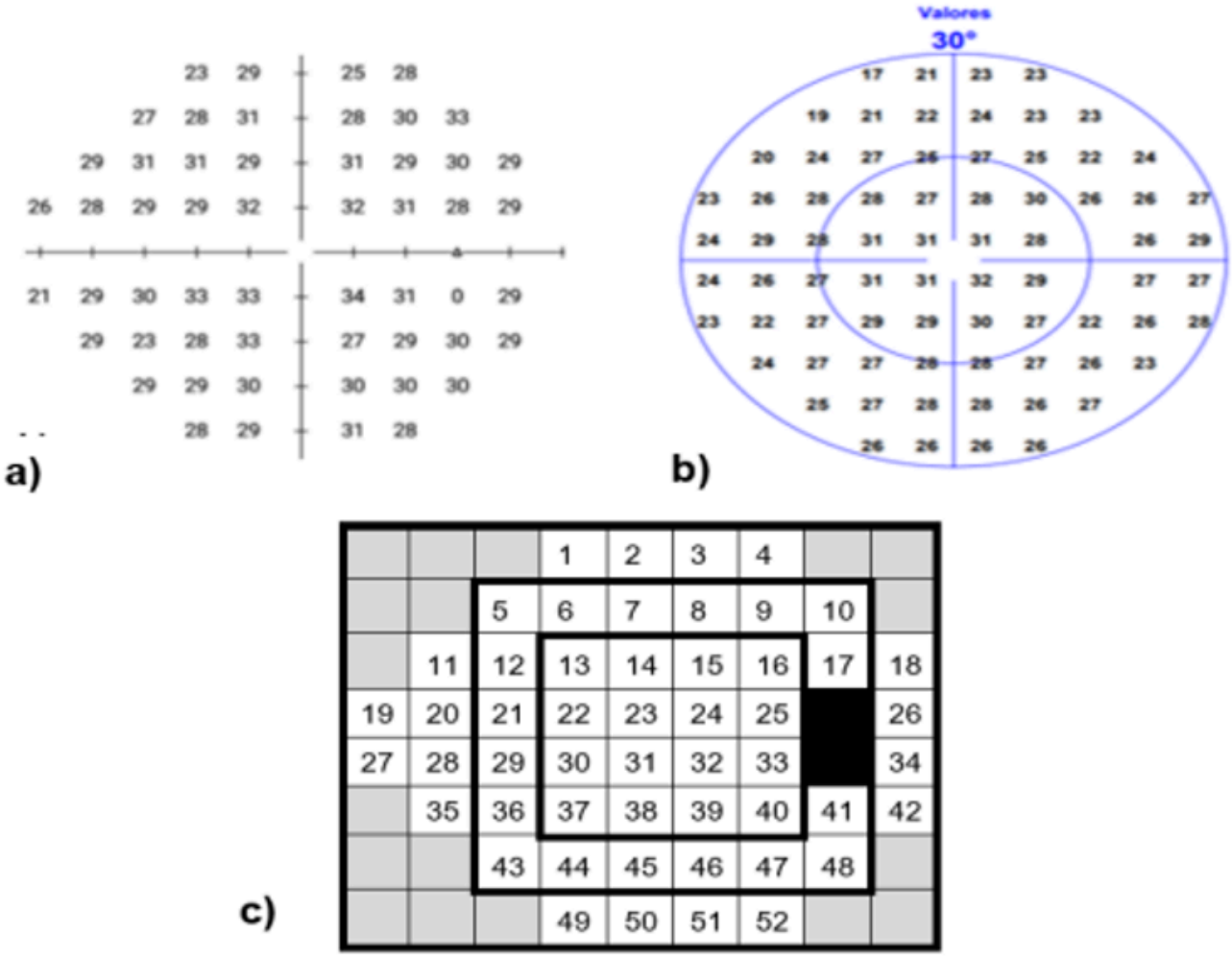


Figure 1

AVA and Octopus visual fields with zonal distribution of study locations

a) Advanced Vision Analyzer, 24-2 pattern (52 locations).

b) Octopus 101 Haag-Streit, 32 pattern.

c) Distribution of the 52 study locations across three eccentricity zones. Zone 0–10° (locations 13–16, 22–25, 30–33, 37–40). Zone 10–20° (5–10, 12, 17, 21, 29, 36, 41, 43–48). Zone 20–30° (1–4, 11, 18–20, 26–28, 34-35, 42, 49–52).

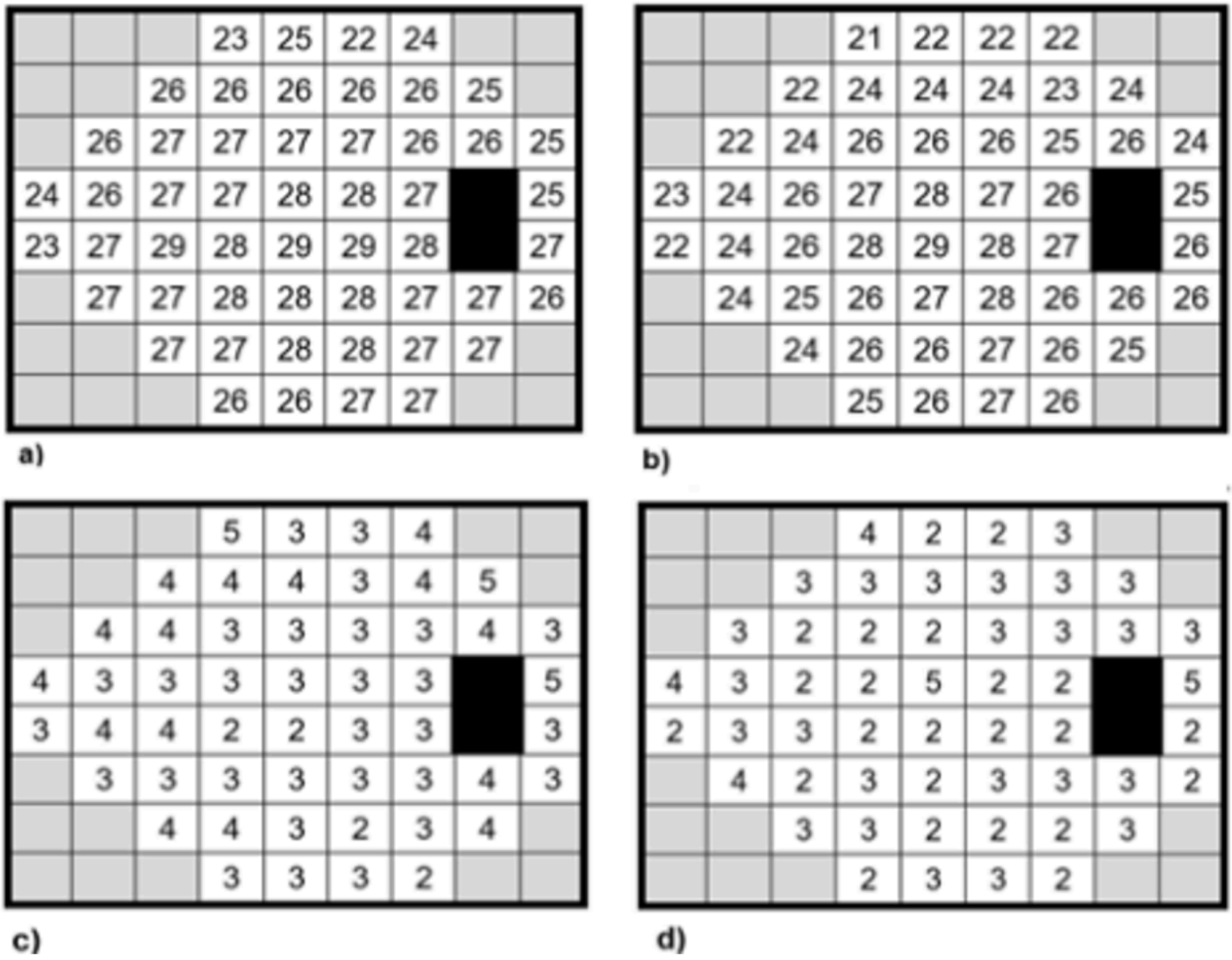


Figure 2

Pointwise mean sensitivity: AVA–Octopus 101 comparison

a) Pointwise mean sensitivity obtained with AVA

b) Pointwise mean sensitivity obtained with Octopus 101

c) Absolute difference in pointwise mean sensitivity (|AVA − Octopus 101|), allowing identification of regions with greater local discrepancy

d) Standard deviation of absolute pointwise differences, reflecting inter-subject variability at each location

The similar pointwise mean sensitivity between AVA and Octopus, with low differences and variability, suggests good agreement in most locations, particularly in central zones. This figure supports the utility of AVA as a functional assessment tool in clinical settings, with no evidence of systematic bias

			0.39	0.51	0.49	0.45		
		0.27	0.44	0.29	0.45	0.47	0.18	
	0.52	0.51	0.46	0.57	0.45	0.43	0.67	0.51
0.32	0.60	0.19	0.48	0.58	0.50	0.51		0.43
0.43	0.57	0.64	0.72	0.64	0.60	0.21		0.42
	0.55	0.54	0.63	0.78	0.65	0.50	0.23	0.50
		0.61	0.79	0.71	0.62	0.42	0.58	
			0.63	0.43	0.28	0.64		

- rho 0.70-0.89; p<0.001; Sig.
- rho 0.40-0.69; p<0.05; Sig.
- rho < 0.39; p>0.05

			0.62	0.75	0.71	0.65		
		0.37	0.61	0.37	0.62	052	0.50	
	0.73	0.73	0.59	0.68	0.60	0.64	0.69	0.72
0.38	0.73	0.50	0.68	0.54	0.67	0.68		0.39
0.73	0.72	0.63	0.85	0.80	0.68	0.47		0.65
	0.82	0.77	0.73	0.83	0.76	0.74	0.34	0.58
		0.74	0.72	0.81	0.73	0.53	0.73	
			0.75	0.49	0.33	0.77		

- ICC > 0.75; p<0.05; Sig.
- ICC 0.50-0.75; p<0.05; Sig.
- p>0.05

Figure 3

Pointwise mean sensitivity: AVA–Octopus 101 agreement

a) Spearman correlation coefficients (rho): strong and moderate significant correlations (black and blue) predominated between both technologies, particularly in the central zone.

b) Intraclass correlation coefficients (ICC): moderate to high correlations (ICC > 0.50) with statistical significance were observed in most locations, supporting consistency between the two technologies.

Note: Non-significant locations (a and b) may be associated with anatomical variability, glaucomatous damage, reduced peripheral precision, or specific characteristics of the virtual reality environment.

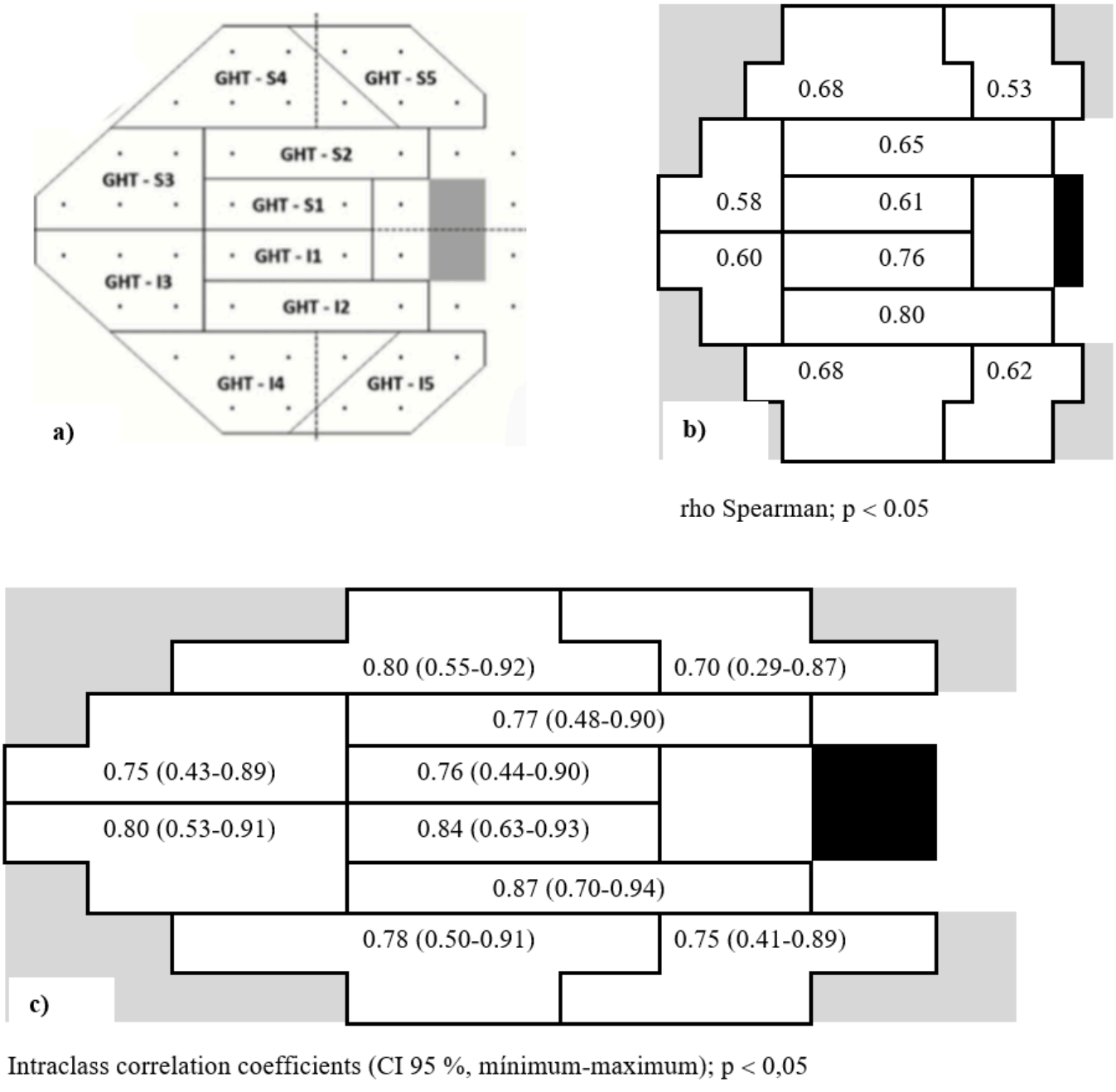


Figure 4

Mean sensitivity in sectors of the Glaucoma Hemifield Test: AVA–Octopus 101

a) Representation of the GHTsectors in the right eye, according to Asman and Heijl (31).

b) A predominance of moderate–strong correlations was observed between measurements from both perimeters, with the highest values in inferior sectors 1 and 2 (rho = 0.76–0.80). The lowest correlation occurred in superior sector 5 (rho = 0.53). These findings support the functional validity of the AVA algorithm compared to the Octopus standard

c) Intraclass correlation coefficients for each of the ten functional GHT sectors. Elevated and statistically significant values were observed (ICC ≥ 0.70; $p < 0.05$) across all evaluated sectors.

Overall, these results demonstrate robust concordance and functional validity of AVA compared to the Octopus 101 across GHT sectors.